Available online at www.sciencedirect.com
ScienceDirect
Tetrahedron
Tetrahedron 64 (2008) 733–740
www.elsevier.com/locate/tet

On the behaviour of the (*Z*)-phenylhydrazones of some 5-alkyl-3-benzoyl-1,2,4-oxadiazoles in solution and in the gas phase: kinetic and spectrometric evidence in favour of self-assembly

Antonella Fontana [a], Susanna Guernelli [b], Paolo Lo Meo [c], Elisabetta Mezzina [b], Stefano Morganti [b], Renato Noto [c,*], Egon Rizzato [b], Domenico Spinelli [b,*], Romina Zappacosta [a]

[a] *Dipartimento di Scienze del Farmaco, Università ''G. d'Annunzio'', Via dei Vestini 31, 66013 Chieti, Italy*
[b] *Dipartimento di Chimica Organica ''A. Mangini'', Università di Bologna, Via San Giacomo 11, 40126 Bologna, Italy*
[c] *Dipartimento di Chimica Organica ''E. Paternò'', Università di Palermo, Viale delle Scienze, Parco d'Orleans II, pad. 17, 90128 Palermo, Italy*

Received 6 September 2007; received in revised form 16 October 2007; accepted 1 November 2007
Available online 6 November 2007

Abstract

Rate constants, $k_{A,R}$, for the rearrangement of the (*Z*)-phenylhydrazones (**1a–e**) of a series of 5-alkyl-3-benzoyl-1,2,4-oxadiazoles substituted at C(5) with linear alkyl chains of different length (from C_4 up to C_{12}) into the relevant 4-acylamino-2,5-diphenyl-1,2,3-triazoles (**2a–e**) have been measured in dioxan/water in the base-catalyzed region (pS^+ 10.5–12.6). For each substrate log $k_{A,R}$ are linearly related to pS^+. The significant decrease of the slopes of these straight lines (from 0.96 down to 0.78) upon increasing the length of the linear alkyl chain at C(5) and that of the reactivity (down to 14–26%) upon increasing the substrate concentration suggest a decrease of the polarity of the 'actual' reaction medium and provide indirect evidence of the tendency of the substrates (*Z*)-**1a–e** to self-assemble. To confirm the above outcome direct evidence of the formation of self-assemblies in solution were obtained from ^{1}H NMR and spectrofluorimetry measurements while ESI-MS experiments point out the presence of aggregated substrates also in the gas phase.

1. Introduction

Our research group is involved by long time in the kinetic study of the mononuclear rearrangement of heterocycles (MRH) or Boulton–Katritzky reaction (BKR).[1,2]

Our interest in this and in general in ring interconversion of azoles is based on both the intriguing mechanistic aspects of the rearrangement (depending on both the proton concentration and the structure of the investigated substrates) and the wide synthetic applicability of ring interconversion of 1,2,4-oxadiazoles.[1–3] E.g., a strong electron-withdrawing substituent, such as a perfluoroalkyl,[3] favoured new irreversible ring-degenerate rearrangements[3a] as well as new ANRORC-like (*A*ddition of a *N*ucleophile followed by *R*ing *O*pening and *R*ing *C*losure) processes eventually associated with ring-enlargement.[3b–f]

In order to extend the study of the reactivity in MRH of (*Z*)-phenylhydrazones of 3-benzoyl-1,2,4-oxadiazoles, we have synthesized a new series of 5-alkyl-substituted substrates with the aim of evaluating the effect of linear alkyl chains of different lengths (from C_4 up to C_{12}) on the rearrangement rates of (*Z*)-**1a–e** into the relevant triazoles **2a–e** (Scheme 1).

The presence of long linear alkyl chains at C(5) of the 1,2,4-oxadiazole ring could favour self-assembly and consequently could affect the course of the rearrangement. In this paper we will therefore investigate the supramolecular behaviour of the title substrates by collecting evidence on their ability to self-assemble both in solution (by using kinetics,

* Corresponding authors. Tel.: +39 091 596919 (R.N.); tel.: +39 051 2095689; fax: +39 051 2095688 (D.S.).
E-mail addresses: rnoto@unipa.it (R. Noto), domenico.spinelli@unibo.it (D. Spinelli).

0040-4020/$ - see front matter © 2007 Elsevier Ltd. All rights reserved.
doi:10.1016/j.tet.2007.11.014

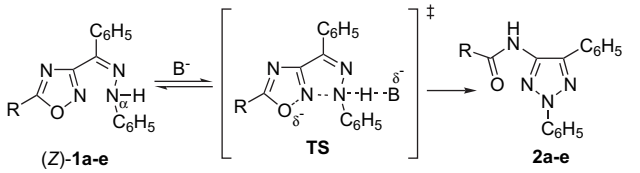

a: R = C_4H_9 **b**: R= C_6H_{13} **c**: R = C_8H_{17} **d**: R = $C_{10}H_{21}$ **e**: R = $C_{12}H_{25}$

Scheme 1. Base-catalyzed rearrangement of the (*Z*)-phenylhydrazones **1a–e** into the relevant triazoles **2a–e**.

^{1}H NMR spectrometry, and spectrofluorimetry) and in the gas phase (by using ESI-MS).

2. Results and discussion

2.1. Kinetic investigation

The rearrangement of (*Z*)-**1a–e** into **2a–e** has been studied in dioxan/water (D/W; 1:1, v/v) at different proton concentrations. The apparent first-order rate constants, $k_{A,R}$, and the corresponding rate profile (plot of log $k_{A,R}$ vs pS^+) are reported in Table S1 of Supplementary data and Figure 1, respectively.

Figure 1 highlights that in the investigated pS^+ range: (a) the reactivity is largely affected by proton concentration as has already been observed for other base-catalyzed MRHs;[2,4,5] (b) all the (*Z*)-phenylhydrazones (**1a–e**) investigated show similar reactivity, e.g., at pS^+ ca. 11.5 the reactivity ratio between the investigated substrates is 1.00±0.15 in line with the mechanism proposed (S_Ni)[2a–d] and the strictly similar electronic effects of the investigated 5-alkyl groups;[2e] (c) only at the lowest and at the highest investigated pS^+ does the reactivity of the five substrates become significantly different, spanning from $(k_{A,R})_{\mathbf{1a}}/(k_{A,R})_{\mathbf{1e}}$ 0.74 up to 1.7 at pS^+ 10.5 and 12.5, respectively.

The slopes of the rate profiles (Fig. 1) decrease from 0.96 down to 0.78 on increasing the length of the linear 5-alkyl chain (Table S1). The rather low slope[4–6] values obtained for (*Z*)-**1d** and (*Z*)-**1e** suggest a tendency of these substrates to self-assemble into clusters of different size. The observed rate constants are probably the outcome of different contributions from mononuclear rearrangement of each aggregated or monomer form of the substrate.

In order to gain more information on the association process we carried out a further kinetic investigation on the MRH at different concentrations of (*Z*)-phenylhydrazone of 3-benzoyl-5-hexyl-1,2,4-oxadiazole (**1b**) (from 3.0×10^{-5} up to 5.0×10^{-4} M), keeping constant the borate buffer concentration. The measured rate constants at different pS^+ values are reported in Table S2 of Supplementary data and the plots of log $k_{A,R}$ versus [(*Z*)-**1b**] at three different pS^+ in Figure 2.

The data in Figure 2 point to an 'apparent' significant decrease, observed for the first time, of the reactivity upon increasing the concentration of (*Z*)-**1b** (14–26% in the pS^+ range 12.1–10.8) up to a critical (*Z*)-**1b** concentration. This reactivity decrease, at each investigated pS^+, could be related to a change in the state of aggregation of the substrate. Above the critical breakpoint concentrations the reactivity reaches a minimum plateau value suggesting that the MRH process is brought about only by a largely prevailing and less reactive substrate self-assembled into an aggregate with an optimum aggregation number. Indeed at this high (*Z*)-**1b** concentration the aggregated form of the substrate should prevail over the monomer form. The breakpoint concentrations depend slightly on the pS^+ value, but anyway (*Z*)-**1b** appears to be completely aggregated above 1×10^{-4} M.

This behaviour of (*Z*)-**1b** well agrees with that observed for the rearrangement of the same substrate in water/β-CD at similar proton concentrations.[2f] In the latter case the much larger decrease (ca. 31) of the rearrangement rate with respect to the reaction in D/W was ascribed to the more hydrophobic environment of the cavity of β-CD compared with D/W solutions. In the present case the long linear chain at C-5 favours the

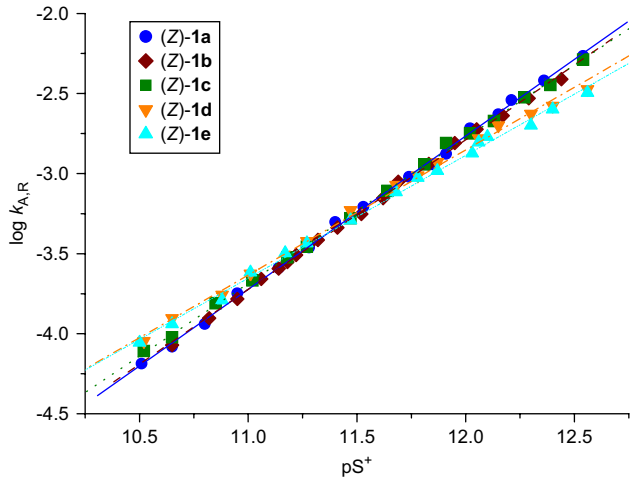

Figure 1. Plot of log $k_{A,R}$ for the rearrangement of (*Z*)-**1a–e** into **2a–e** in D/W at 313 K versus pS^+.

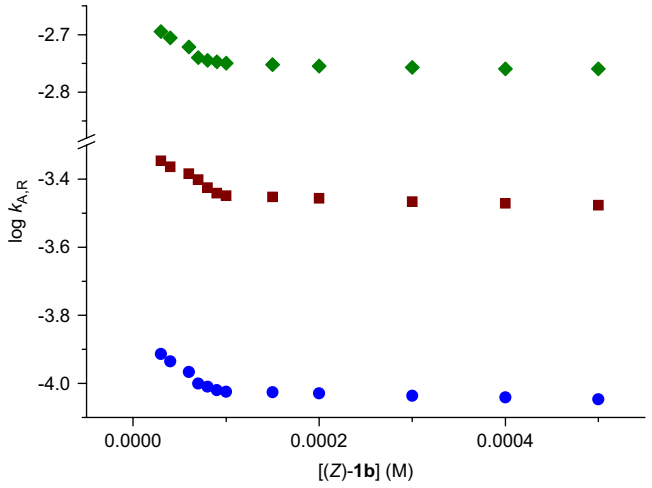

Figure 2. Plot of log $k_{A,R}$ for the rearrangement of (*Z*)-**1b** into **2b** in D/W versus concentration of (*Z*)-**1b** at pS^+ 10.80 (●), 11.38 (■), and 12.10 (◆).

formation of aggregated substrate, which provides a more hydrophobic environment in which the rearrangement takes place.

2.2. Spectrometric evidence for self-assembly

The self-association of (*Z*)-**1a–e** and also of **2a–e** has been studied by ^{1}H NMR and spectrofluorimetry in solution and by ESI-MS in the gas phase. Strong support for the occurrence of self-assembly has been obtained by all the three techniques.

2.2.1. ^{1}H NMR measurements

We examined the ^{1}H NMR behaviour of the only (*Z*)-**1a** (R=C_4H_9) derivative, because of the very low solubility of the other *Z*-phenylhydrazones (**1b–e**) in water. Nevertheless a small amount of CD_3OD (3% v) was added to the D_2O solution in order to ensure the complete sample dissolution. Spectra were recorded at different (*Z*)-**1a** concentrations (from 1×10^{-4} up to 8.0×10^{-4} M) in a wide range of temperature (298–333 K).

By increasing the temperature from 298 to 333 K an improvement of the resolution of all signals of the ^{1}H NMR spectrum of 1.0×10^{-4} M (*Z*)-**1a** solution (Fig. 3) was observed, in agreement with a disaggregation occurring at higher temperature. Figure 3 points out higher shifts for aliphatic protons with respect to the aromatic ones, suggesting that only aliphatic hydrophobic chains are involved in the aggregation process.

To examine whether the aggregation process occurs for both (*Z*)-**1a** and the relevant triazole **2a**, ^{1}H NMR spectra were recorded by using solutions containing increasing fractions of CD_3OD (see Figs. 4 and 5, respectively), a solvent in which the intermolecular interactions are minimized.

As a matter of fact a different effect of the structure of the side chains on the aggregation process could be expected. The substituent bound to the C(5) of the 1,2,4-oxadiazole ring in (*Z*)-**1a** is a linear alkyl chain, which can give only van der Waals interactions. In contrast in **2a** the alkyl chain is bound to the C(4) of the 1,2,3-triazole ring via an amide group, which can give polar (hydrogen bonds and dipole–dipole) interactions with other **2a** molecules or with the solvent. Spectra of the two compounds were also measured in pure CD_3OD in order to obtain data for the non-aggregated molecule (upper traces of Figs. 4 and 5).

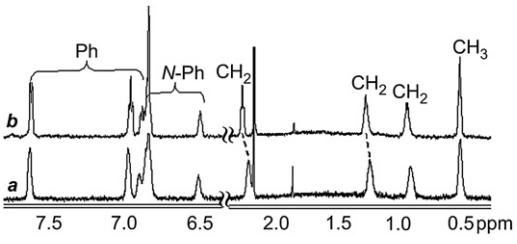

Figure 3. Spectrum of a 1.0×10^{-4} M solution of (*Z*)-**1a** in D_2O/CD_3OD (97:3) at: (a) 298 K; (b) 333 K.

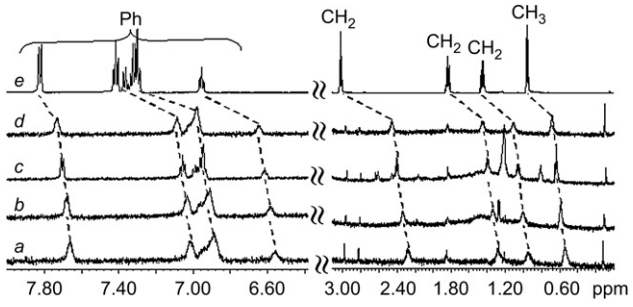

Figure 4. ^{1}H NMR spectra of a 1.1×10^{-4} M solution of (*Z*)-**1a** recorded at *T* 298 K in solution of D_2O/CD_3OD (v/v): (a) 10:1, (b) 4:1, (c) 2.5:1, (d) 1.7:1, (e) 0:1.

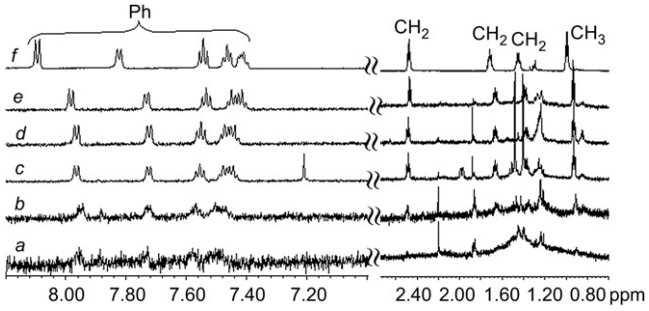

Figure 5. ^{1}H NMR spectra of a 1.2×10^{-4} M solution of **2a** recorded at *T* 298 K in solution of D_2O/CD_3OD (v/v): (a) 6:1, (b) 4:1, (c) 1.5:1, (d) 1.2:1, (e) 1:1.75, (f) 0:1.

Marked upfield shift (red dotted lines) and broadening of both aromatic and aliphatic signals can be observed for (*Z*)-**1a** on decreasing the fraction of CD_3OD (see spectra a–d of Fig. 4).

The behaviour of **2a** is quite different (Fig. 5): its aromatic and aliphatic signals appear more and more resolved on going from spectrum a to e, while neither marked shifts nor broadening of the peaks are observed. The signals maintain their spin–spin couplings even at a high concentration of D_2O where the signal-to-noise ratio is less favourable (spectrum a). It is quite evident that triazole **2a** does not self-assemble in solution in these experimental conditions, notwithstanding the presence of the alkyl chain. The polar amido group favours the solvation with water or methanol (via hydrogen bonds[7]) over substrate–substrate interactions.

Our findings concerning (*Z*)-**1a** and **2a** (R=C_4H_9) could be reasonably extended at least to short chain derivatives. Moreover our experiments do not exclude the self-assembly in solution of triazoles with longer alkyl chains as it has been detected in the gas phase where the absence of solvent molecules allows only substrate–substrate interactions (see below).

2.2.2. Spectrofluorimetric measurements

The tendency of (*Z*)-**1b** and (*Z*)-**1e** (R=C_6H_{13} and $C_{12}H_{25}$, respectively) to self-assemble was tested also through spectrofluorimetry by using 9-diethylamino-5*H*-benzo[α]phenoxazin-5-one (Nile Red) as the fluorescent probe. The solvatochromic fluorescent probe Nile Red has already been proved to be very

efficient in its capability to identify different aggregate morphologies formed by amphiphilic mixtures.[8]

Spectra were recorded at different concentrations of the investigated (*Z*)-phenylhydrazones (from 1.9×10^{-8} up to 5.5×10^{-4} M) at 298 K (data at increasing concentrations of (*Z*)-**1b** are reported in Fig. S1 of Supplementary data). The fluorescence intensity rises with increasing [(*Z*)-**1b**] and the maximum emission wavelength, λ_{max}, exhibits a remarkable blue shift [from 648 to 582 nm for (*Z*)-**1b** (Fig. 6a and Fig. S1 of Supplementary data) and from 648 to 575 nm for (*Z*)-**1e** (Fig. S2 of Supplementary data)].

The cac (*c*ritical *a*ggregation *c*oncentration) can be evaluated either at the onset of the fluorescence intensity increase in the plot of fluorescence intensity emission versus log [substrate][8a] or at the inflection point in the plot of λ_{max} versus log [substrate][8b] (Fig. 6a and b, respectively).

The average cac calculated are 3×10^{-5} and 5×10^{-5} M for (*Z*)-**1b** and (*Z*)-**1e**, respectively. Figure 6b shows a not very steep transition from the λ_{max} of the monomer to that of the aggregate covering an interval of [(*Z*)-**1b**] of about 2 orders of magnitude. This effect reveals that the observed phenomenon is not a simple aggregation process from monomers to micelles but a rather more complex transformation of substrate into different aggregates (i.e., dimers, trimers and eventually small clusters).

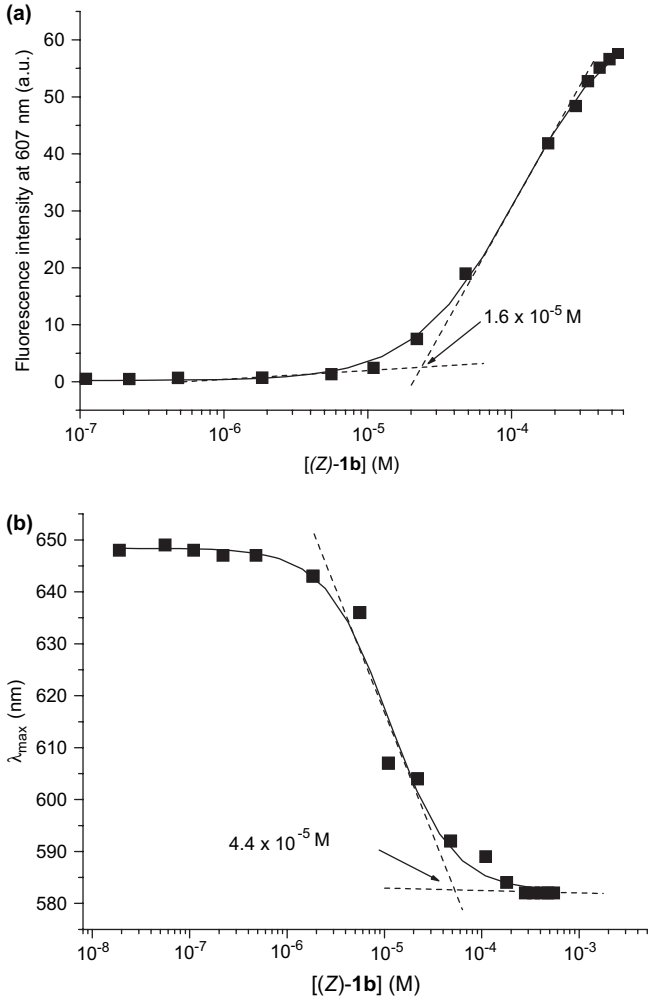

Figure 6. (a) Plot of the fluorescence intensity (arbitrary units) versus the concentration of (*Z*)-**1b**. (b) Plot of the λ_{max} (nm) versus the concentration of (*Z*)-**1b**.

As a matter of fact, classical techniques, used for the cmc (*c*ritical *m*icellar *c*oncentration) determination, such as tensiometry[9] and solubilization of water insoluble dye-molecules,[9] were not able to provide evidence for the formation of true micelles (data not shown). It is generally accepted that cmc strongly depends on the length of the hydrophobic group.[9] In contrast the C_6H_{13}-substituted (*Z*)-**1b** appears to have comparable cac values. This suggests that aggregates of different type and dimensions are obtained from the two substrates.

2.2.3. ESI-MS measurements

Interestingly, direct evidence for self-assembly for all the investigated compounds [(*Z*)-**1a–e** and **2a–e**] have been obtained by electrospray ionization mass spectrometry (ESI-MS). Several recent literature examples have been reported on the use of ESI-MS measurements to detect and evaluate self-association processes in the gas phase.[10–12] In an ESI-MS analysis, charged species (host–guest complexes or self-assembly systems) are transferred from the small droplets of solution into gas phase under relatively mild conditions, generally without fragmentation.[13] The principal problem in using ESI-MS in supramolecular chemistry is to determine whether the peaks present in the spectra correspond to species present in solution, or whether these peaks are the result of processes occurring in the mass spectrometer. If this problem is solved, for example, by comparing data obtained with ESI-MS and data obtained with other independent techniques, ESI-MS data can give new information on the supramolecular behaviour of the system.

The ESI-MS spectra were recorded in positive ion mode with a variation of the concentration of the substrate, **S**, from 1.0×10^{-6} up to 2.0×10^{-4} M [**S** dissolved in water/acetonitrile (1:1, v/v)]. All the spectra showed the molecular ion peak and a high-intensity signal corresponding to the dimer $(\mathbf{S})_2$. On increasing [**S**] a weak, double charged signal corresponding to the trimer $(\mathbf{S})_3$ was also observed.

In Figure 7a and b the spectra of **2b** at 3.0×10^{-6} M and 1.1×10^{-4} M, respectively, are reported as examples of the general behaviour displayed by all the examined compounds. Figure 7a shows the presence of different peaks ascribable to the monocharged monomer {*m*/*z*=349, 371, 412 corresponding to $[\mathbf{2b}+H]^+$, $[\mathbf{2b}+Na]^+$ and $[\mathbf{2b}+\text{acetonitrile}+Na]^+$, respectively} and dimer {*m*/*z*=719 corresponding to $[(\mathbf{2b})_2+Na]^+$}. At higher substrate concentrations the peak of the double charged trimer $[(\mathbf{2b})_3+K+H]^{2+}$ (at *m*/*z*=542) is also detected.

The monotonic increase of $(\mathbf{S})_2$ with increasing [**S**] {the peak corresponding to the dimer going from 25% at [**2b**]=3.0×10^{-6} M (Fig. 7a) up to 100% at [**2b**]=1.1×10^{-4} M (Fig. 7b)}, the significant detection of trimers only at the highest [**S**] (Fig. 7b) and the appearance of the same peaks at all the investigated cone voltage (from 20 to 80 V,

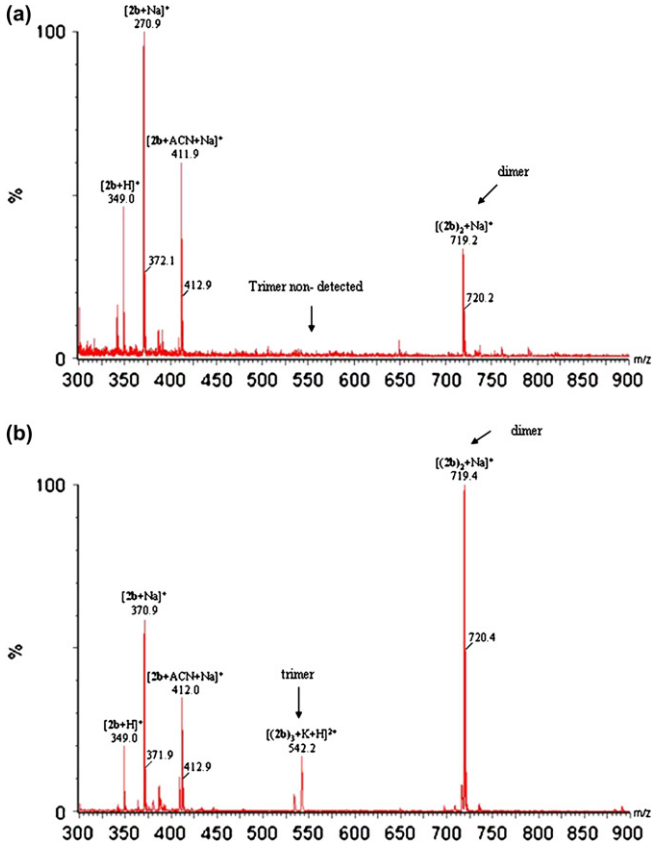

Figure 7. (a) ESI-MS spectrum of a 3.0×10^{-6} M solution of **2b** in water/acetonitrile (1:1, v/v); ACN: acetonitrile. (b) ESI-MS spectrum of a 1.1×10^{-4} M solution of **2b** in water/acetonitrile (1:1, v/v); ACN: acetonitrile.

data not shown) suggest that the detected species are not artifacts formed in the mass spectrometer during the measurement but rather correspond to species already present in solution.[14,15]

The absence of any evidence of aggregation in the instance of the parallelly studied **2a** from ^{1}H NMR measurements could be due therefore to the solvation ability towards **2b** of the CD_3OD/D_2O mixtures with respect to the situation observed by ESI-MS in the gas phase (i.e., in the absence of solvents).

In order to confirm the ability of the studied **S** to self-associate, the ESI-MS spectra of **2b** were recorded in the presence of CTAB (at concentration below its cmc) in ion positive mode at increasing [**2b**]. The peak intensity at m/z=632 (deriving from a 1:1 association between the cationic surfactant and **2b**) increases with increasing [**2b**] (data in Table 1) and eventually becomes the base peak. Thus, **2b** shows a high tendency to aggregate only (see the above reported ^{1}H NMR data concerning **2a**) with molecules with a remarkable lipophilic domain (e.g., CTAB contains a linear alkylic chain of 16 carbon atoms).

Recently, the binding constants of both small organic host–guest complexes or large biological complexes have been determined[16–18] by ESI-MS as the relative abundances of the complexes detected by this technique have been proved[16] to correlate with the equilibrium distribution in solution. For example ESI-MS has been used to measure the association

Table 1
Major peaks and relative abundance of the ESI-MS spectra of **2b** in the presence of cetyltrimethylammonium bromide, CTAB

Molar ratio CTAB:**2b**	Major peak observed[a]	Relative abundance (%)
1:0.2	632.4 $[CTA\cdot\mathbf{2b}]^+$	50
	649.4 $[CTAB+CTA]^+$	100
	719.4 $[(\mathbf{2b})_2+Na]^+$	Trace
	735.3 $[(\mathbf{2b})_2+K]^+$	Trace
1:0.5	632.4 $[CTA\cdot\mathbf{2b}]^+$	100
	649.4 $[CTAB+CTA]^+$	48
	719.2 $[(\mathbf{2b})_2+Na]^+$	Trace
	735.3 $[(\mathbf{2b})_2+K]^+$	Trace
1:1	632.4 $[CTA\cdot\mathbf{2b}]^+$	100
	649.4 $[CTAB+CTA]^+$	46
	719.3 $[(\mathbf{2b})_2+Na]^+$	Trace
	735.3 $[(\mathbf{2b})_2+K]^+$	Trace

[a] The peak corresponding to the heterodimers lacks a bromide ion, accordingly the signals of the dimer of the surfactant correspond to species with only one bromide ion (in table, CTA: cetyltrimethylammonium ion).

constants of glycopeptide antibiotics, which form both homo and heterodimers.[14,15] The validity of this method relies on the assumption that the ionization probability of the monomer should be similar to that of the dimer for every compound. Moreover the published[15] good agreement between dimerization constants determined by ESI-MS and those acquired in solution by other independent and complementary methods (e.g., ^{1}H NMR) demonstrates that the ESI-MS spectra reflect, at least qualitatively, the real stability of the complex in solution.

Nevertheless we determined the dimerization constants for **S** from only ESI-MS measurement with the main aim of comparing the stability of the dimer for the different investigated compounds and aware of the fact that the obtained equilibrium constants refer to the experimental conditions adopted for the ESI-MS measurement, the studied equilibrium being:

$$\mathbf{S}+\mathbf{S}\rightleftharpoons(\mathbf{S})_2 \qquad (1)$$

The equilibrium concentrations of **S** and $(\mathbf{S})_2$ were calculated from the sum of the ion abundances (measured by peak areas) of all the monomeric and dimeric forms, respectively. The apparent dimerization constants, K_{dim}, were calculated by Eq. 2.

$$K_{dim}=\frac{[(\mathbf{S})]_2}{[\mathbf{S}]^2} \qquad (2)$$

The K_{dim} values for (*Z*)-**1a–e** and **2a–e** were estimated at low concentration of **S** (1.0×10^{-5} M for 1,2,4-oxadiazoles and 2.0×10^{-6} M for 1,2,3-triazoles) in order to avoid the formation of trimers: their values are reported in Table 2 and give information concerning the trend of dimer stability as a function of the structure of **S**.

Interestingly, the triazoles **2a–e** showed a greater ability to give dimers, with association constants 6–15 times higher than those of the oxadiazoles (*Z*)-**1a–e**. As expected, K_{dim} values of (*Z*)-**1** and **2** increase on increasing the linear alkyl chain length. The effect is particularly strong for the longest

Table 2
Dimerization constants[a] of (*Z*)-**1a–e** and **2a–e**

S	K_{dim}[b] (M^{-1})
1a	5.4×10^3
1b	6.0×10^3
1c	7.2×10^3
1d	1.5×10^4
1e	2.2×10^4
2a	6.9×10^4
2b	8.1×10^4
2c	8.9×10^4
2d	9.4×10^4
2e	3.2×10^5

[a] The values were averaged over 10 experiments recorded at different concentration of **S**.
[b] The errors were estimated to be approximately 15%.

alkyl chain derivatives [(*Z*)-**1d**, (*Z*)-**1e**, and **2e**], whereas K_{dim} values are very similar for those with shorter alkyl chains [see K_{dim} values for (*Z*)-**1a–c** and **2a–d**].

The dependence of K_{dim} on linear alkyl chain length at C(5) in (*Z*)-**1a–e** indicates that the van der Waals interactions must contribute significantly to the self-assembling, particularly for the derivatives with the longest alkyl chains. However, dimers from triazoles **2a–e** turn out to be more stable than oxadiazole dimers suggesting that intermolecular hydrogen bonds, particularly strong for amides,[7] can significantly contribute to K_{dim}.

3. Conclusions

Rate constants for MRH of (*Z*)-phenylhydrazones of a series of 5-alkyl-3-benzoyl-1,2,4-oxadiazoles **1a–e** with linear alkyl chains of significantly different length (from C_4 up to C_{12}) at the same pS^+ are only slightly different, in agreement with the similar electronic and the negligible steric effects of linear alkyl chains of different length. It had already been proved[2e] that the rearrangement rates of the (*Z*)-phenylhydrazones of some 5-alkyl-3-benzoyl-1,2,4-oxadiazoles (alkyl= Me, Et, ^{i}Pr and ^{t}Bu) in D/W are only moderately affected by the substituent of the 1,2,4-oxadiazole ring.

An interesting outcome obtained from kinetic data is the significant decrease of the slope values of the lines obtained by plotting the logarithmic rate constants versus pS^+ (from 0.96 down to 0.76) on going from the substrate with the shortest alkyl chain (C_4), (*Z*)-**1a**, to the substrate with the longest alkyl chain (C_{12}) at C(5), (*Z*)-**1e**. This decrease appears to be indicative of a variation in the polarity of the microenvironment in which the rearrangement process takes place and therefore of the tendency of the (*Z*)-**1a–e** to self-assemble. Indeed, slopes significantly lower than unity indicate that the base-catalyzed rearrangement does occur in a medium less polar than the hydrophilic D/W mixture.[2,4–6]

A further confirmation of the formation of aggregated substrates comes from the first time observed dependence of the $k_{A,R}$ of the investigated MRH on the (*Z*)-**1b** concentration.

Direct evidence for self-assembly of the examined (*Z*)-phenylhydrazones (**1a–e**) of 3-benzoyl-5-alkyl-1,2,4-oxadiazoles both in solution and in the gas phase have been obtained by ^{1}H NMR, spectrofluorimetry, and ESI-MS measurements. Association constants, obtained by ESI-MS analysis, provide qualitative information about the specific interactions, not easily detectable in solution, involved in the dimerization processes of the different (*Z*)-**1a–e** and **2a–e** and allow to differentiate the contributions of the linear alkyl chains and of the amide group to the aggregation phenomena.

On the whole the combined kinetic and spectrometric study has provided evidence of the self-assembly in both (*Z*)-**1a–e** and **2a–e**.

4. Experimental

4.1. General

Synthesis and characterization of 5-alkyl-3-benzoyl-1,2,4-oxadiazoles (**A–E**), (*E*)- and (*Z*)-phenylhydrazones of 5-alkyl-3-benzoyl-1,2,4-oxadiazoles (**1a–e**), and the relevant triazoles (**2a–e**) are reported in Supplementary data. HRMS were recorded on a Thermo Finnigan Mat95XP apparatus.

4.2. General procedure for the synthesis of 5-alkyl-3-benzoyl-1,2,4-oxadiazoles

5-Alkyl-3-benzoyl-1,2,4-oxadiazoles (**A**, **C–E**) were prepared through the reactions of phenylglyoxyloyl chloride oxime (ω-chloroisonitrosoacetophenone) and the respective oximes (pentanal, heptanal, nonanal, undecanal, and tridecanal oximes) in refluxing toluene according to literature.[19] The crude product of reaction was purified by chromatography on silica gel (elution with a gradient ranging from 98:2 to 90:10 petroleum ether/ethyl acetate). The yields (not optimized) of the pure ketones ranged between 20 and 30%.

4.3. General procedure for the synthesis of the (*E*)- and (*Z*)-phenylhydrazones of 5-alkyl-3-benzoyl-1,2,4-oxadiazoles (*1a, c–e*)

The title compounds were prepared and purified according to the methods reported.[2c–f] Phenylhydrazine (8 mmol) was added to a solution of 5-alkyl-3-benzoyl-1,2,4-oxadiazole (4 mmol) and acetic acid (0.2 mL) in ethanol (80 mL). The mixture was kept at room temperature in the dark. After 48 h the ethanol solution was concentrated at reduced pressure to a small volume and the residue extracted with ethyl ether. The combined ethereal extracts were washed repeatedly with water, dried with sodium sulfate and evaporated at reduced pressure. The residue was chromatographed on silica gel (eluted with a gradient ranging from 98:2 to 90:10 petroleum ether/ethyl acetate) to give the (*Z*)- and, in case, the (*E*)-isomer.

4.4. Heat-induced rearrangement of the (*Z*)-phenylhydrazones (*1a, c–e*) into triazoles (*2a, c–e*)

Thermally induced rearrangement of (*Z*)-**1a**, **c–e** gave **2a**, **c–e** by heating the samples (0.2 g) in a preheated oil-bath

(150 °C) for a few minutes. By purification on a silica gel column (petroleum ether/ethyl acetate 85:15) triazoles were obtained in practically quantitative yields.

4.5. Kinetic measurements

The kinetics in D/W (1:1, v/v) were followed spectrophotometrically as previously described[2c–f] by measuring the disappearance of (*Z*)-**1a–e** at the wavelengths of their absorption maxima, where the absorptions of the relevant triazoles **2a–e** were negligible. An operational pH scale, pS^+,[2c] was established in aqueous dioxan by employing the pK_a values of acids determined by interpolation from the data reported by Harned and Owen.[20] For D/W (1:1, v/v) the pH-meter reading after calibration against buffers was not significantly different from pS^+, requiring a correction of only +0.16.

Pseudo-first-order conditions were ensured by using a large excess of borate buffer (1.25×10^{-2} M); the concentration of (*Z*)-**1a–e** was 5.00×10^{-5} M. Kinetic measurements for (*Z*)-**1b** were carried out at variable substrate concentration (from 3.0×10^{-5} to 5.0×10^{-4} M). The spectrophotometric measurements were collected with a double-beam spectrophotometer (Varian Cary 1E). The rate constants are accurate within ±3%.

4.6. NMR measurements

^{1}H and ^{13}C NMR spectra of all synthesized compounds were carried out on spectrometers (Varian Gemini) operating at 300 (proton) and 75.5 MHz (carbon) or at 200 and 50 MHz for proton and carbon, respectively, using the solvent peak as internal reference. Chemical shifts are reported in parts per million (δ scale).

1D and 2D NMR spectra were recorded on spectrometers operating at 600 or at 400 MHz (Varian Mercury). In order to completely solubilize the substrate, the ^{1}H NMR experiments were performed in mixed solutions of D_2O/CD_3OD using residual HOD as an internal standard (4.76 ppm at 298 K).

ROESY data were collected on a Varian spectrometer operating at 600 MHz, using a 90° pulse width of 6.1 μs and a spectral width 6000 Hz in each dimension, respectively. The data were recorded in the phase sensitive mode using a CW spin-lock field of 2 KHz, without spinning the sample. Acquisitions were recorded at mixing times 100–500 ms. Other instrumental settings are: 128 increments of 2K data points, 32–64 scans per t_1, 1.5 s delay time for each scan.

4.7. Fluorimetric measurements

Steady-state emission spectra were recorded on a spectrofluorimeter Jasco FP-6200, with a band-pass of 5 nm and an excitation λ=550 nm. Aqueous solutions (5.0×10^{-7} M) of the fluorescent probe Nile Red were used for all the measurements.

On addition of different aliquots of a mother solution of the oxadiazoles (*Z*)-**1b** and (*Z*)-**1e** in dioxan to the aqueous solution of Nile Red, fluorescence emission remained very low up to a critical aggregation concentration (cac).[8] The formation of aggregates from (*Z*)-**1b** and (*Z*)-**1e**, into which Nile Red preferentially solubilizes, was confirmed also by the blue shift of the λ_{max} of Nile Red observed at similar oxadiazole concentrations.

4.8. ESI-MS measurements

ESI-MS spectra were acquired with a single quadrupole mass spectrometer. A syringe driven by a pump was used for direct injection of the sample into the instrument (ZMD Micromass single quadrupole operating at *m*/*z*=4000). Changing the cone voltage from 80 to 20 V did not change significantly the absolute intensity of the peaks.

To minimize the influence of variations in instrumental conditions on the reliability of mass spectra, the ESI-MS parameters (i.e., the pressure of the gas, the desolvation temperature, the capillary and cone voltages, etc.) were kept rigorously constant from run to run in each series of experiments. In particular a capillary voltage of 2.70 kV and a cone voltage of 20 V were applied; a desolvation temperature of 150 °C was used.

The solutions of (*Z*)-**1a–e** and **2a–e** in acetonitrile/water (1:1, v/v) were introduced at a flow-rate of 15 μL min^{-1}. For the determination of dimerization constants the errors were estimated to be approximately 15%. For the measurements with surfactant a cone voltage of 30 V was applied. The values of relative abundance were averaged at least from 10 independent experiments.

In the experiments with CTAB the monomeric surfactant gave very intense signals that could mask the peaks of other species present in the solution. We have therefore examined the spectral range *m*/*z*=330–750, renormalizing the relative abundance. In every case mass spectra were averaged over typically 50 scans.

Acknowledgements

The authors thank M.I.U.R. (Rome) [PRIN 2005 (2005034305) and PRIN 2006 (2006034372)] for the financial supports. Investigations supported also by the Universities of Bologna and Palermo (ex-60%, funds for selected research topics).

Supplementary data

Kinetic constants for MRH of compounds **1a–e**, fluorescence emission spectra of Nile Red on increasing the concentration of (*Z*)-**1b**, plot of the fluorescence intensity versus the concentration of (*Z*)-**1e**. Plot of the λ_{max} (nm) versus the concentration of (*Z*)-**1b**, characterization and ^{1}H NMR spectra of investigated compounds are provided. Supplementary data associated with this article can be found in the online version, at doi:10.1016/j.tet.2007.11.014.

References and notes

1. (a) Boulton, A. J.; Katrizky, A. R.; Hamid, A. *J. Chem. Soc. C* **1967**, 2005–2007; (b) Boulton, A. J. *Lectures in Heterocyclic Chemistry*; Hetero

Corporation: Provo, UT, July 1973; (c) Afridi, A. S.; Katrizky, A. R.; Ramsden, C. A. *J. Chem. Soc., Perkin Trans. 1* **1976**, 315–320; (d) Katrizky, A. R.; Gordev, M. F. *Heterocycles* **1993**, *35*, 483–518; (e) Van der Plas, H. C. *Ring Transformations of Heterocycles*; Academic: London, 1973; Vols. 1 and 2; (f) L'Abbè, G. *J. Heterocycl. Chem.* **1984**, *21*, 621–638.

2. (a) Ruccia, M.; Vivona, N.; Spinelli, D. *Adv. Heterocycl. Chem.* **1981**, *29*, 141–169; (b) Vivona, N.; Buscemi, S.; Frenna, V.; Cusmano, G. *Adv. Heterocycl. Chem.* **1993**, *56*, 49–154; (c) Cosimelli, B.; Frenna, V.; Guernelli, S.; Lanza, C. Z.; Macaluso, G.; Petrillo, G.; Spinelli, D. *J. Org. Chem.* **2002**, *67*, 8010–8018; (d) Bottoni, A.; Frenna, V.; Lanza, C. Z.; Macaluso, G.; Spinelli, D. *J. Phys. Chem. A* **2004**, *108*, 1731–1740; (e) Frenna, V.; Vivona, N.; Consiglio, G.; Spinelli, D. *J. Chem. Soc., Perkin Trans. 2* **1984**, 541–545; (f) Guernelli, S.; Lo Meo, P.; Morganti, S.; Noto, R.; Spinelli, D. *Tetrahedron* **2007**, *63*, 10260–10268.
3. (a) Buscemi, S.; Pace, A.; Pibiri, I.; Vivona, N.; Lanza, C. Z.; Spinelli, D. *Eur. J. Org. Chem.* **2004**, 974–980; (b) Buscemi, S.; Pace, A.; Pibiri, I.; Vivona, N. *J. Org. Chem.* **2002**, *67*, 6253–6255; (c) Buscemi, S.; Pace, A.; Pibiri, I.; Vivona, N.; Spinelli, D. *J. Org. Chem.* **2003**, *68*, 605–608; (d) Buscemi, S.; Pace, A.; Pibiri, I.; Vivona, N.; Caronna, T. *J. Fluorine Chem.* **2004**, *125*, 165–173; (e) Buscemi, S.; Pace, A.; Palumbo Piccionello, A.; Macaluso, G.; Vivona, N.; Spinelli, D.; Giorgi, G. *J. Org. Chem.* **2005**, *70*, 3288–3291; (f) Buscemi, S.; Pace, A.; Palumbo Piccionello, A.; Pibiri, I.; Vivona, N.; Giorgi, G.; Mozzanti, A.; Spinelli, D. *J. Org. Chem.* **2006**, *71*, 8106–8113.
4. Frenna, V.; Vivona, N.; Consiglio, G.; Corrao, A.; Spinelli, D. *J. Chem. Soc., Perkin Trans. 2* **1981**, 1325–1328.
5. D'Anna, F.; Frenna, V.; Macaluso, G.; Marullo, S.; Morganti, S.; Pace, V.; Spinelli, D.; Spisani, R.; Tavani, C. *J. Org. Chem.* **2006**, *71*, 5616–5624.
6. Laidler, K. J. *Chemical Kinetics*; McGraw-Hill: London, 1965; pp 450–463.
7. Le Questel, J.-Y.; Laurence, C.; Lechkar, A.; Helbert, M.; Berthelot, M. *J. Chem. Soc., Perkin Trans. 2* **1992**, 2091–2094.
8. (a) Coutinho, P. J. G.; Castanheira, E. M. S.; Rei, M. C.; Elisabete, M.; Oliveira, C. D. R. *J. Phys. Chem. B* **2002**, *106*, 12841–12846; (b) Stuart, M. C. A.; van de Pas, J. C.; Engberts, J. B. F. N. *J. Phys. Org. Chem.* **2005**, *18*, 929–934; (c) Seliskar, C. J.; Brand, L. *J. Am. Chem. Soc.* **1971**, *93*, 5414–5420.
9. Clint, J. H. *Surfactant Aggregation*; Chapman and Hall: New York, NY, 1992; pp 82–129.
10. Schmuck, C.; Wienand, W. *J. Am. Chem. Soc.* **2003**, *125*, 452–459 and references therein.
11. (a) Manet, I.; Francini, L.; Masiero, S.; Pieraccini, S.; Spada, G. P.; Gottarelli, G. *Helv. Chim. Acta* **2001**, *84*, 2096–2107; (b) Haino, T.; Fujii, T.; Fukazawa, Y. *J. Org. Chem.* **2006**, *71*, 2572–2580.
12. Guernelli, S.; Laganà, M. F.; Mezzina, E.; Ferroni, F.; Siani, G.; Spinelli, D. *Eur. J. Org. Chem.* **2003**, 4765–4776.
13. (a) Cech, N. B.; Enke, G. E. *Mass Spectrom. Rev.* **2001**, *20*, 362–387; (b) Schalley, C. A. *Int. J. Mass Spectrom.* **2000**, *194*, 11–39; (c) Kebarle, P.; Tang, L. *Anal. Chem.* **1993**, *65*, 972A–986A; (d) Kebarle, P. *J. Mass Spectrom.* **2000**, *35*, 804–817.
14. Jørgensen, T. J. D.; Roepstorff, P.; Heck, A. J. R. *Anal. Chem.* **1998**, *70*, 4427–4432.
15. Staroske, T.; O'Brien, D. P.; Jørgensen, T. J. D.; Roepstorff, P.; Williams, D. H.; Heck, A. J. R. *Chem.—Eur. J.* **2000**, *6*, 504–509.
16. Kempen, E. C.; Brodbelt, J. S. *Anal. Chem.* **2000**, *72*, 5411–5416.
17. Oshovsky, G. V.; Verboom, W.; Fokkens, R. H.; Reinhoudt, D. N. *Chem.—Eur. J.* **2004**, *10*, 2739–2748.
18. Zhan, Y.; Meng, C.; Cunyu, Y.; Fengrui, S.; Zhiqiang, L.; Shuying, L. *Rapid Commun. Mass Spectrom.* **2007**, *21*, 683–690.
19. Sasaki, T.; Yoshioka, T.; Suzuki, Y. *Bull. Chem. Soc. Jpn.* **1971**, *44*, 185–189.
20. (a) Bates, R. G. *Solute–Solvent Interactions*; Coetze, J. F., Ritchie, C. D., Eds.; Marcel Dekker: New York, NY, 1969; p 46; (b) Harned, H. S.; Owen, B. B. *The Physical Chemistry of Electrolytic Solution*, 3rd ed.; ACS Monograph No. 137; Reinhold: New York, NY, 1970; pp 755, 716.